Transactions of the Materials Research Society of Japan 32[2] 531-534 (2007)

Development and characterization of thermoelectron enhanced microplasma devices for the generation of plasmas in micro-sized capillaries

Sven Stauss, Hiroyuki Miyazoe, Masaki Sai, and Kazuo Terashima

Department of Advanced Materials Science, Graduate School of Frontier Sciences, The University of Tokyo
5-1-5 Kashiwanoha, Kashiwa-shi, Chiba-ken, 277-8561 Japan
Fax: +81-4-7136-3798, *e*-mail: kazuo@plasma.k.u-tokyo.ac.jp

Microplasmas offer the advantage of small size, low power consumption as well as higher rate of materials processing and are therefore promising for new applications in materials processing. While many different types of microplasma devices have been presented in recent years, the effects of the smaller scale on the properties of the plasma (gas and electron temperatures), distribution of electrons, radicals and ions, and the implications of these characteristics for materials processing have not been studied in detail yet. Here we present the generation and characterization by optical emission spectroscopy (OES) as well as the numerical simulation of atmospheric pressure argon microplasmas inside capillaries with inner diameters between 50 μm and 1 mm using two different types of thermoelectron enhanced microplasma (TEMP) devices. The first type has a freestanding geometry whereas the second type is planar, fabricated by a surface mount technique. The latter allows for future size reduction of the microplasma setup and for an easier integration with other apparatuses and devices.

Keywords: microplasma, microcapillaries, surface mounted microplasma device

1. INTRODUCTION

Because of their small size and low energy consumption, microplasma sources are very attractive for materials treatment and different types of microplasma sources with various designs have been presented by Hopwood *et al.* [1], Ito and Terashima [2] and Ichiki *et al.* [3]. Besides their evident attractivity for processing of new materials [4] and for localized treatment/deposition of semiconductors [5, 6], metals [7] and polymers [8, 9], their small size also allows for miniaturization of existing scientific instruments [10] or an easy integration with other devices.

The power necessary to ignite and sustain the plasma can be reduced considerably if the plasma device is equipped with a thermoelectron source [2]. One of the main aims of this work is to further reduce the size of this type of microplasma source, in order to benefit from its advantageous properties which are a low power consumption and a high plasma density. However, the original geometry of the TEMP device is freestanding, which makes further miniaturization difficult.

To lift the difficulties related to the assembly of the original configuration, we have developed a new setup and fabrication method where the components of the microplasma torch are surface mounted using a reflow technique. Because of the planar layout, the size of the TEMP device can eventually be further miniaturized and be integrated more easily into other apparatus such as scanning electron microscopes (SEM) or other devices, e.g. micro-electromechanical systems (MEMS) or microfluidic components. In order to assess the characteristics of the microplasma and to obtain a better understanding of the effect of the reduced size on the plasma properties, optical emission spectroscopy measurements (OES) as well as computational fluid dynamics (CFD) simulations were conducted. The experimental setup of the thermoelectron enhanced microplasma (TEMP) and fabrication method of the surface mounted microplasma device are presented in section 2, while the experimental and numerical results are presented and discussed in section 3.

2. EXPERIMENTAL

The experimental setup for the TEMP is represented in Fig. 1. The microplasma is generated inside a capillary into which a tungsten filament is inserted. A metallic tube is wound around the capillary and the electromagnetic field is generated by applying an ultra high frequency (UHF) signal of 450 MHz to this solenoid coil. By applying a high voltage (HV) of 15 kV to the tungsten filament for a period of 0.6 seconds, electrons are emitted from its tip by field enhanced thermionic emission (FEE), permitting to ignite the plasma.

The central part of the setup consists of a solenoid coil made of a copper tube (cf. Fig. 1(b). The elements of the matching network are directly soldered on the copper tubes, permitting to reduce the size of the circuit and to increase power efficiency into the coil. One factor determining the value of the resonant frequency f_0, besides the values of the capacitors C_0 and C_1 is the geometry of the solenoid coil. Slight changes of the geometry (inner diameter of the coil, distance between turns of the coil), caused for instance by Joule heating, result in a shift of f_0. The copper tube allows for cooling the circuit by gas or water and therefore to stabilize f_0. Fabricating the coil is quite time consuming and not very reproducible. Because of the difficulties with the freestanding microplasma torch, a modified version, permitting a surface mount assembly of coil and matching circuit was devised.

A simplified equivalent circuit of the matching network which acts as a bandpass filter is shown in Fig. 2(a). In practice, at very high frequencies effects such as current losses to the substrate as well as additional resistances, ca-

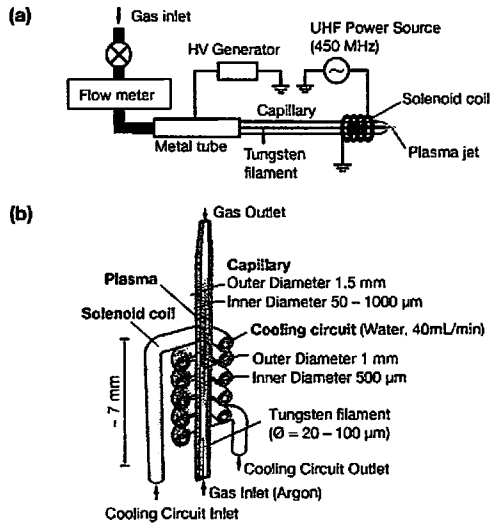

Fig. 1 (a) Schematic description of the thermoelectron enhanced microplasma consisting of a UHF (450 MHz) power generator, a high voltage source (15 kV) and a solenoid coil out of copper which is wound around a capillary. A tungsten filament is inserted into the capillary and serves as thermoelectron source. The gas-flow is controlled by a gas flow meter (after Ref. [2]). (b) Geometry of the solenoid coil used for the generation of the plasma.

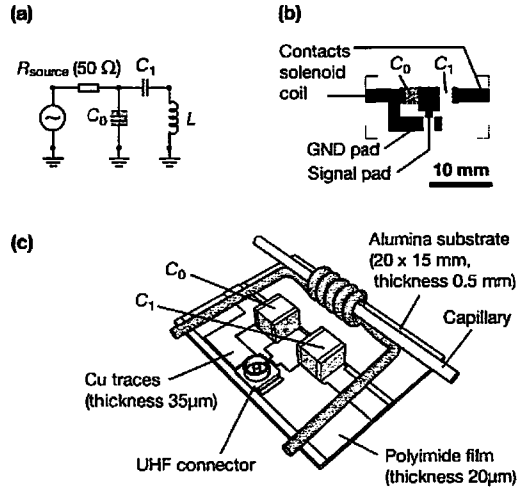

Fig. 2 (a) Simplified equivalent circuit of the matching network (b) surface layout of circuit (c) Schematic illustration of final assembled microplasma device.

pacitances and inductances due to the contact of the components to the circuit board have to be taken into account. Fig. 2(b) shows the layout of the circuit. The support of the circuit consists of a flexible polyimide film (thickness 20 μm) and a copper layer (thickness 35 μm. The lines and solder pads of the matching circuit are structured by a laser assisted photolithography process. The polyimide film is then bonded to an alumina substrate. Solder paste (ECO solder, Senju Metal Industries, Co. Ltd, Japan) is applied on the solder pads using a syringe. Then the components are placed on the designated pads. The whole board and components are heated at a temperature of 190°C for 5 minutes, after which the substrate is brought to the melting temperature of the solder of 240°C for a few seconds. Misplaced components are drawn to the destined places by the surface tension of the solder. Fig. 2(c) shows a schematic of the final assembled circuit.

Two types of microcapillaries were used: The first type possessing a straight geometry were fused silica capillaries (Polymicro Technologies, LLC, USA) with an outer diameter of 367 μm and inner diameters of 50, 75 and 100 μm. For capillary diameters of 500 and 1000 μm, quartz glasses were used (Sutter Instrument Co., USA). The second type of capillaries was fabricated by using a micropipette puller (P-2000, Sutter Instrument Co., USA) which allowed to adjust the geometry of the nozzle. The diameter of the tungsten filament inserted into the capillaries was 20 μm for the capillaries with inner diameters of 50 and 75 μm, 50 μm for the 100 μm capillaries and 100 μm for the 500 μm and 1 mm capillaries.

In these experiments, a microplasma power generator system (Nihon Koushuha Co. Ltd., Japan), where the HV unit and UHF generator are integrated in one unit, was used. The UHF signal is fixed at a frequency of

Table 1 Gas flow rates of argon and N_2 as well as input and reflected powers used for plasma generation. Prior to ignition, the Tungsten filament was heated during a period of 3-6 min. at an input power $P_{in} = 9$ W. Argon input pressure $p_{Ar} = 2$ atm.

D (μm)	D_W (μm)	$\dot{m}$(Ar) (slm)	P_{in} (W)	P_r (W)
50	20	0.2	25.0	0.1 – 0.3
75	20	0.2	25.0	~ 0
100	50	0.2	25.0	0 – 0.1
500	100	0.4	25.0	0.4 – 0.7
1000	100	0.4	25.0	0.5 – 0.6

450 MHz and the input power can be adjusted between 0.3 and 30 W. The matching frequency of the circuit before and after operation of the microplasma was verified by a spectrum analyzer (R3131A, Advantest Co. Ltd., Japan). Optical emission spectra (OES) of the generated microplasma were acquired by a spectrometer (Acton Research Instruments Co. Ltd., USA).

The microplasma jets were generated under atmospheric conditions with an argon input pressure of $p = 2$ atm. After a short preheating period of 3 to 6 minutes of the tungsten filament, the plasma was ignited at a power of 25 W. The detailed experimental conditions of applied powers and gas flow rates $\dot{m}$ are listed in Tab. 1. For the estimation of the gas temperature T_g, N_2 was mixed with Ar, ($\dot{m}(N_2) = 1$ sccm, for both $\dot{m}$(Ar) = 0.2 slm and $\dot{m}$(Ar) = 0.4 slm).

For the moment, only coarse OES measurement with respect to the size of the capillaries could be conducted. T_g was estimated from the rotational temperature T_{rot} of N_2 determined from the second positive system of N_2 using the method proposed by Phillips [11].

In order to better understand the influence of the capillary size on the plasma properties, computational fluid dynamics (CFD) simulations were conducted using a commercial code, CFD-ACE+ [12]. The simulations were conducted by solving the coupled problem of heat transfer, fluid mechanics, species reactions and transport as

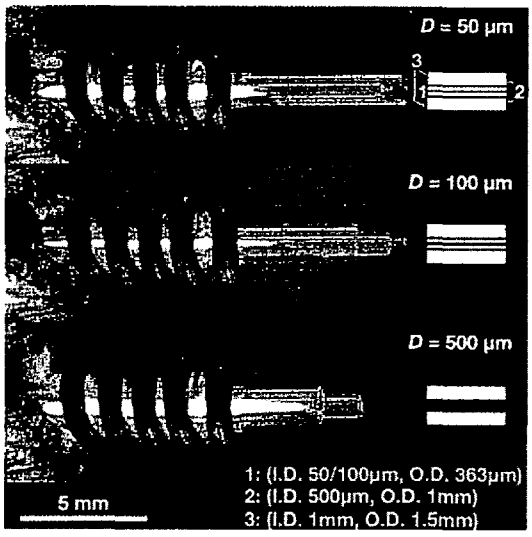

Fig. 3 Microplasma jets generated inside fused silica microcapillaries (freestanding geometry of matching network). The tungsten filament needed for igniting the plasma and as an electron source is positioned at the centre of the first turn of the coil from the left. To increase the mechanical stability of the microcapillaries, they are inserted into other capillaries with bigger inner diameter, as indicated in the right part of the figure.

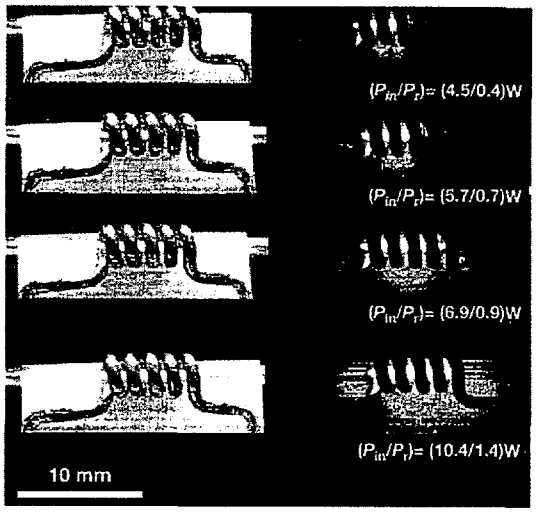

Fig. 4 Microplasma generation with the surface mounted TEMP generated at absolute input powers ($P_{in} - P_r$) between 4 and 9 W.

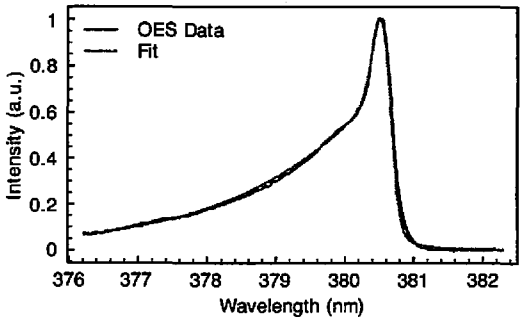

Fig. 5 OES data of the N_2 second positive system and numerical fit for capillary with $D = 500\,\mu m$. Estimated value of $T_g = 1080 \pm 50\,K$.

well as electromagnetics, but does not take into account the effect of the electrons emitted by FEE. The details pertaining to the simulation (volume and boundary conditions, reactions between species) will be described elsewhere [13]. In order to account for the atmospheric pressure conditions, besides electron-atom interactions (elastic, excitation to metastable levels and ionization of Ar), also three-body mechanisms as well as surface reactions (to take into account electron loss at the capillary surface) were included.

3. RESULTS

Photographs of the microplasma jets generated in microcapillaries with inner diameters of 50, 100, and 500 μm are shown in Fig. 3. The right part of Fig. 3 shows the relative size of the different capillaries. The tungsten filament is positioned in the centre of the first turn from the left of the solenoid coil.

Microplasma jets generated using the surface mounted TEMP are depicted in Fig. 4. Here, the tip of the tungsten filament was inserted in the centre of the third turn of the solenoid coil. Using this new type of assembly, the plasmas could be generated at input powers of 9 W and sustained at input power as low as 4 W. At input powers below 10 W, a stable microplasma can be sustained and cooling by convection of the ambient air is sufficient to keep the resonant frequeny f_0 constant. For low input powers and when the resonant frequency f_0 of the circuit could be adjusted to exactly 450 MHz, the reflected power P_r was zero. For higher input powers, the reflected power increased, which can be attributed to increasing mismatch between matching network and source caused by heating of the plasma system. Therefore for higher input powers of 12 W and more, this setup cannot be operated without active cooling.

Fitting of the optical emission spectra of the second positive system of N_2 revealed a variation of the gas temperature between about 900 and 1100 K, with decreasing values of T_g for reduced capillary diameters. For these first series of gas temperature acquisition, compared to the capillary size a relative coarse optical probe having a diameter of the optical fibre $D = 3.175$ mm was used, therefore the spatial resolution of these measurements is poor and the estimated temperatures have to be treated as average values.

The results of the CFD simulations are described in the following paragraph. The geometry of the simulation model is shown in the upper part of Fig. 6, with the temperature field of two capillariy sizes of $D = 1$ and 5 mm for three different levels of absorbed power of 5, 10 and 20 W. For both geometries, T_g increases with increasing power. In contrast to the large model, in the smaller model the region where $T_g \sim 1200$ K is confined to a very small region below the middle coil. It can also be seen that for the same input power, T_g decreases for smaller capillary

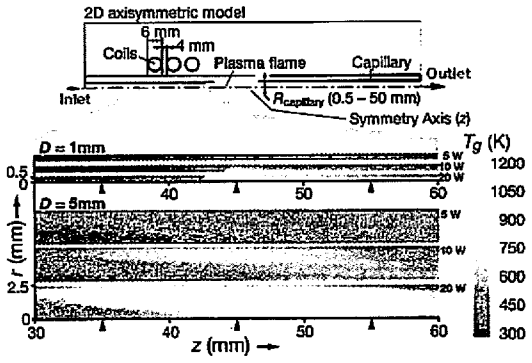

Fig. 6 Axisymmetric model used for the CFD simulations and distribution of T_g in a region below the coils. The upward arrows ▲ indicate the positions of the coils along the z-axis.

sizes. We assume that for smaller capillaries, as the specific volume decreases, the heat capacity of the gas is diminished, resulting in lower values of T_g as well as higher confinement of regions with high T_g.

The results of the numerical simulations also show that the intensity of the electromagnetic field decreases towards the centre of the capillary. Therefore, for a constant coil diameter but decreasing inner capillary diameter, the energy of the electromagnetic field is less efficiently transferred to the gas, making the ignition and stable generation of the plasma more difficult. This could also be verified experimentally as it become more difficult to ignite the plasma as the diameter of the capillary decreased and without the use of an additional electron source, ignition and sustainment of the plasma seems not to be possible [2]. One solution to this problem without resolving to higher input powers would be to reduce the diameter of the coil.

However, plasma ignition using reduced nozzle type microcapillaries revealed to be easier and could also be conducted at lower power values. Ichiki *et al.* [14] also used two types of capillaries with reduced nozzles and reported that the shape of the nozzle has a pronounced effect on the electron density, n_e. It could be that in straight capillaries, the electron density is lower and therefore ignition and sustainment of the plasma are more difficult in such geometries, compared to where the nozzle diameter is reduced. However, a direct comparison of straight and reduced capillary geometries has not been conducted yet.

4. CONCLUSIONS

In this report, the successful generation of microplasmas in straight microcapillaries with inner diameters down to 50 μm was shown. Assessment of T_g from OES measurements suggest gas temperatures between 900 and 1100 K, decreasing for smaller capillaries. Because of the small size of the plasmas, the temperature distributions of both T_g and T_e inside the plasma, could not be evaluated yet. From numerical simulations it is however concluded that for smaller capillary sizes, that the microplasma deviates more and more from the local thermodynamic equilibrium (LTE). In order to be able to generate a microplasma more easily inside these microcapillaries, a modified, planar type of the original microplasma torch geometry was devised. This setup also permits a more integrated as well as a more reproducible assembly of the circuit and therefore to obtain more accurate matching to the required frequency f_0. Another advantage of bringing the matching network close to the antenna by reducing its size is that power losses in the circuit can be reduced. In order to improve the stability of the surface mounted microplasma device and to avoid the necessity of an active cooling circuit, it is suggested to directly pattern the conductive traces onto the dielectric substrate.

We view this type of microplasma source as promising for selective materials processing (etching as well as deposition). Furthermore, the planar assembly of the microplasma source should allow for further size reduction and therefore an easier integration with other apparatuses and devices.

Acknowledgments

The authors acknowledge the help from Takaaki Tomai and Ken Ogata and Think Laboratory, Co. Ltd., Japan, for the fabrication of the film type circuits. This project is funded by the Japanese Society for the Promotion of Science (JSPS), Grant No. P05101.

References

[1] J. A. Hopwood, *Journal of Microelectromechanical Systems* **9**, 309 (2000).
[2] T. Ito and K. Terashima, *Applied Physics Letters* **80**, 2648 (2002).
[3] T. Ichiki, T. Koidesawa, and Y. Horiike, *Plasma Sources Science & Technology* **12**, S16 (2003).
[4] Y. Shimizu, T. Sasaki, T. Ito, K. Terashima, and N. Koshizaki, *Journal of Physics D-Applied Physics* **36**, 2940 (2003).
[5] T. Ideno and T. Ichiki, *Thin Solid Films* **506–507**, 235 (2006).
[6] H. M. L. Tan, T. Ideno, and T. Ichiki, *Journal of Photopolymer Science and Technology* **18**, 237 (2005).
[7] Y. Shimizu, T. Sasaki, A. C. Bose, K. Terashima, and N. Koshizaki, *Surface & Coatings Technology* **200**, 4251 (2006).
[8] Y. Shimizu, T. Sasaki, K. Terashima, and N. Koshizaki, *Journal of Photopolymer Science and Technology* **19**, 235 (2006).
[9] H. M. L. Tan, T. Akagi, and T. Ichiki, *Journal of Photopolymer Science and Technology* **19**, 245 (2006).
[10] O. B. Minayeva and J. A. Hopwood, *Journal of Analytical Atomic Spectrometry* **17**, 1103 (2002).
[11] D. M. Phillips, *Journal of Physics D* **9**, 507 (1976).
[12] ESI-Group, *CFD-ACE+* (2006), URL `http://www.esi-group.com/SimulationSoftware/CFD_ACE/`.
[13] S. Stauss, H. Miyazoe, M. Sai, and K. Terashima (In Preparation).
[14] T. Ichiki, R. Taura, and Y. Horiike, *Journal of Applied Physics* **95**, 35 (2004).

(Received January 5, 2007;Accepted January 11, 2007)